 

# Gas Transport Coefficients of Light Hydrocarbons. Halogenated Methane and Ethane as Candidates for New Refrigerants

**Jalil Moghadasi,[1] Mohammad Mehdi Papari,*[2] Delara Mohammad-Aghaie,[1] and Antonio Campo[3]**

[1]Department of Chemistry, College of Sciences, Shiraz University, Shiraz 71454, Iran

[2]Department of Chemistry, Shiraz University of Technology, Shiraz 71555-313, Iran

[3]Department of Mechanical Engineering, The University of Vermont, Burlington, VT 05405, USA

Received April 10, 2007; E-mail: papari@sutech.ac.ir

In previous work, we have correlated the dilute gas transport properties of alternative refrigerant mixtures. The purpose of this theoretical study was to obtain, using two-iterative inversion of the corresponding states of viscosity, effective and isotropic pair potential energies for a group of refrigerants: methane, ethane, propane, butane, R22, R123, R124, R134a, R152a, R32, and R143a. Employing the inverted pair potential energies, the Chapman–Enskog scheme could be used reasonably well to reproduce transport properties, except the thermal conductivity. The thermal conductivity was determined using the Huber scheme, wherein the use of the inverted pair potential energies is discussed at length. In the wide temperature range of $200\,\mathrm{K} < T < 1000\,\mathrm{K}$, the accuracies of the calculated viscosities, self-diffusion coefficients, and thermal conductivities were 2%, 4%, and 8% (at most 10%), respectively.

Hydrocarbon molecules are important in a plethora of fields spanning from biological systems to intricate processes in the chemical industry. In the latter, hydrocarbons are employed as feedstocks for the production of natural gas, petrochemicals, gasoline, kerosene, oil, and paraffin wax.

Pure refrigerants and refrigerant mixtures are widely used as working fluids in industrial applications involving refrigerators and heat pumps. For example, difluorochloromethane (R22), 1,1,1,2-tetrafluoroethane (R134a), and 1,1-difluoroethane (R152a) are used as pure blend components for refrigeration purposes. R134a and R152a are also propellants for aerosol and blowing agents for extruded polystyrene foams. Therefore, knowledge of the transport properties of this kind of refrigerant has paramount importance in the design and fabrication of these devices. Such knowledge is also of theoretical relevance, because it provides a legitimate framework for the understanding of intermolecular forces acting in refrigerant systems.[1] However, direct measurement of the pertinent thermophysical properties over a wide range of temperatures and pressures is impractical. In the past decades, a great amount of effort has been devoted to the development of procedures for estimating thermophysical properties. These procedures mostly based on rigorous theory are sample supported by accurate measurements in carefully chosen scenarios.

During the last two decades, new high-performance refrigerants, known as hydrochlorofluorocarbons (HCFCs) and hydrofluorocarbons (HFCs), have merged as the result of intense and rapid technological developments.[2] For the development of alternative refrigerant fluids, the primary concern is ozone depletion and global warming with the hope of reducing greenhouse gas emissions.[3] HCFCs have shorter atmospheric lifetimes than CFCs and deliver less reactive chlorine to the stratosphere, where the "ozone layer" is found. In light of this, it is expected that these chemicals will be more benign to the stratospheric ozone than CFCs. Because HCFCs contain chlorine, they yet have the potential to destroy stratospheric ozone. As a result, HCFCs are only viewed as temporary replacements for CFCs.

Second-generation replacements of CFCs are known as hydrofluorocarbons (HFCs). HFCs have been categorized by the worldwide industry and the scientific community as ozone-safe alternatives to CFCs and HCFCs, because as HFCs contain no chlorine, these gases do not affect the stratospheric ozone directly. Furthermore, some mechanisms for ozone destruction, caused by fragments produced as HFCs decompose within the atmosphere, i.e., $CF_3$ radicals, have been shown to be insignificant.

In previous works, Papari and his co-workers have successfully determined the transport properties of refrigerant mixtures,[4] polyatomic molecules[5–7] as well as the thermodynamic properties of refrigerants and refrigerant mixtures.[8,9] The aim of present work was to predict dilute gas transport properties of refrigerants, encompassing a wide range of temperatures. This was done by determining effective and isotropic pair potential energies for the studied refrigerants from corresponding states correlation of viscosity using the inversion method. In this study, the alternative refrigerants considered were HCFCs, including R22, R123, R124, and HFCs, including R134a, R152a, R143a, and R32. Moreover, the dilute gas transport properties of pure methane, ethane, propane, and butane, considered to be a third class of refrigerants, were calculated. Specifically, we employed the methods proposed by Huber et al.[10,11] to predict the thermal conductivity of these refrigerants. The Chapman–Enskog version of the kinetic theory of gases[12] could be used to determine the remaining transport properties, including the viscosity coefficient, self-diffusion coefficient, and isotopic thermal diffusion factor. The predicted viscosity agrees with experimental measurements to within 2% in

Published on the web February 12, 2008; doi:10.1246/bcsj.81.220

the temperature range of 200 K < $T$ < 1000 K, and the estimates of the thermal conductivity were accurate to within 8% (and at most 10%) in the temperature range of 200 K < $T$ < 1000 K.

## Transport Coefficients

Fundamentally, transport coefficients describe the process of relaxation to equilibrium from a state perturbed by application of temperature, pressure, density, and velocity or composition gradients. The importance of this revolves around the fact that the knowledge of transport properties of materials is a crucial in an immense variety of engineering design calculations.

From a scientific point of view, precise knowledge of transport properties at low density is essential for the development of accurate theories of transport properties in the dense state. In addition, the values of the transport properties of gases are the macroscopic manifestation of the microscopic motions and interactions of the molecules that comprise the gas. Therefore, invoking kinetic theory of gases, the characteristics of the bulk gases, such as transport properties, are related to the properties of individual molecules that make up the gas and the forces existing between them.[13] As a consequence, once the intermolecular forces are known, all of the dilute gas properties can be calculated at any arbitrary temperature even if they have not all been measured. In addition, it is expected that accurate measurements of the transport properties of gases might be used to determine the forces acting between a pair of molecules.

In the present work, we attempted to meet the two major scopes cited before. First, effective and isotropic reduced pair interaction energy for each refrigerant was established from the low-density viscosity data using an inversion method. Thereafter, the calculated pair interaction potential was used to determine other transport properties in a wide range of temperatures. It should be mentioned that, at low density, the viscosity is almost independent of the existence of internal degrees of freedom and is therefore nearly unaffected by inelastic collisions. Thereby, this particular property is one of the most reliable sources for establishing intermolecular potential energies.

The Chapman–Enskog solution of the Boltzmann transport equation[12] supplies expressions for the transport properties of pure gases and their multi-component mixtures at low densities in terms of collision integrals represented by $\Omega^{(l,s)}$. Here, the superscripts $l$ and $s$ appearing in $\Omega$, denote weighting factors that account for the transport mechanism by molecular collision. For example, for the two transport properties viscosity and diffusion, the superscripts have values of $l = 2$, $s = 2$ and $l = 1$, $s = 1$ respectively. The collision integrals are related to the intermolecular forces by the following relations:

$$\theta = \pi - 2b\int_{r_m}^{\infty} \frac{r^{-2}\mathrm{d}r}{\left\{1 - \left(\frac{b^2}{r^2}\right) - \left[\frac{2u(r)}{mw^2}\right]\right\}^{1/2}}, \tag{1}$$

$$Q^{(l)}(E) = 2\pi\left[1 - \frac{1 + (-1)^l}{2(1+l)}\right]^{-1}\int_0^{\infty}(1 - \cos^l\theta)b\mathrm{d}b, \tag{2}$$

$$\Omega^{(l,s)}(T) = [(s+1)!(kT)^{s+2}]^{-1}\int_0^{\infty} Q^{(l)}(E) \times \exp(-E/kT)E^{s+1}\mathrm{d}E, \tag{3}$$

where $\theta$ is the scattering angle, $Q^{(l)}(E)$ the transport collision integral, $b$ the impact parameter, $E$ the relative kinetic energy of colliding partners, $w$ the relative velocity of colliding molecules, $r_m$ the closest approach of two molecules, and $kT$ the molecular thermal energy. Once a definitive expression for the intermolecular force law has been chosen, these integrals can be evaluated numerically. For the case of a pure gas, viscosity and self-diffusivity are given by:

$$\eta = \frac{5}{16}\left(\frac{mkT}{\pi}\right)^{1/2}\frac{f_\eta}{\sigma^2\Omega^{*(2,2)}}, \tag{4}$$

$$D = \frac{3}{8}\frac{(kT/\pi m)^{1/2}}{\rho\sigma^2\Omega^{*(1,1)}}f_D, \tag{5}$$

where

$$f_\eta = 1 + \frac{3}{196}(8E^* - 7)^2, \tag{6}$$

$$f_D = 1 + (1/8)(6C^* - 5)^2/(2A^* + 5). \tag{7}$$

In the preceding equations, the reduced collision integral, $\Omega^{*(l,s)}$ may be defined as:

$$\Omega^{*(l,s)} = \frac{\Omega^{(l,s)}}{\pi\sigma^2}, \tag{8}$$

where $\sigma$ is a characteristic diameter of the molecules, often called the collision diameter or the length scaling factor, such that $u(\sigma) = 0$. The reduced collision integrals are weak functions of reduced temperatures, $T^*$, which are equivalent to:

$$T^* = kT/\varepsilon. \tag{9}$$

In this ratio, $\varepsilon$ denotes the energy scaling factor or the maximum energy of attraction between a pair of molecules. Representative values of the two parameters, $\sigma$ and $\varepsilon$, are known for many substances.

In Eqs. 4 to 7, m stands for molecular mass and $A^*$, $C^*$, and $E^*$ are collision integral ratios defined by the expressions:

$$A^* = \frac{\Omega^{*(2,2)}}{\Omega^{*(1,1)}}, \tag{10}$$

$$C^* = \frac{\Omega^{*(1,2)}}{\Omega^{*(1,1)}}, \tag{11}$$

$$E^* = \frac{\Omega^{*(2,3)}}{\Omega^{*(2,2)}}. \tag{12}$$

Other collision integral ratios, which may become necessary for calculating transport properties, are:

$$B^* = \frac{[5\Omega^{*(1,2)} - 4\Omega^{*(1,3)}]}{\Omega^{*(1,1)}} \tag{13}$$

$$F^* = \frac{\Omega^{*(3,3)}}{\Omega^{*(1,1)}}. \tag{14}$$

It is noteworthy that, although given equations for the viscosity and diffusion are formulated for monatomic gases, they

are also applicable to polyatomic gases. The reason for this is that, in the equations of conservation of mass and momentum for a collision between polyatomic molecules, the center of mass coordinates is more important than the internal coordinates. The Chapman–Enskog version of the kinetic theory of gases[12] applies strictly to molecules that have no internal degrees of freedom. Polyatomic molecules differ not only because they interact through non-spherically symmetric intermolecular pair potentials, but they also possess internal degrees of freedom in the form of rotational and vibrational modes of motion. Since the viscosity and the diffusion coefficients include transporting momentum and mass, they have no bearing on internal degrees of freedom. In view of this, the Chapman–Enskog theory retains its useful form, but collision integrals must be averaged over all possible relative orientations occurring in the collisions.

Mason and Monchick[14] have proposed a simplification of this treatment. The Mason–Monchick collision integrals are given as:

$$\langle \Omega^{(2,2)}(T) \rangle = \frac{1}{4} \int_0^\infty \int_0^{2\pi} \int_0^\infty \gamma^6 \{(1 - \cos^2 \varphi) b \mathrm{d}b \mathrm{d}b \mathrm{d}\psi\} \times \exp(-\gamma^2) \mathrm{d}\gamma^2, \tag{15}$$

where $\gamma = (m/2kT)^{1/2} w$ and $\psi$ is the azimuthal angle. For the sake of brevity, we used the notation $\Omega^{*(l,s)}$ instead of $\langle \Omega^{*(l,s)} \rangle$ in the present paper.

The temperature gradients can cause mass fluxes through a process known as thermal diffusion. The isotopic thermal diffusion factor, $\alpha_0$, is computed by using the Eq. 16:[15]

$$\alpha_0 = \frac{15}{2} \frac{(6C^* - 5)(2A^* + 5)}{A^*(16A^* - 12B^* + 55)} (1 + \kappa_0), \tag{16}$$

$$\kappa_0 = \frac{1}{9}(7 - 8E^*) \left[ \begin{array}{l} \dfrac{2A^*}{(35/4) + 7A^* + 4F^*} \left( H^* + \dfrac{[A^*(7 - 8E^*) - 7(6C^* - 5)][(35/8) + 28A^* - 6F^*]}{42A^*(2A^* + 5)} \right) \\ -\dfrac{5}{7} \left( H^* + \dfrac{7}{5} \dfrac{(6C^* - 5)}{(2A^* + 5)} - \dfrac{3}{10}(7 - 8E^*) \right) \end{array} \right], \tag{17}$$

where

$$H^* = (3B^* + 6C^* - 35/4)(6C^* - 5)^{-1}. \tag{18}$$

In order to extend calculations to the thermal conductivity of polyatomic molecules, the theory of transport properties must account for inelastic collisions. We know that in binary collisions between polyatomic molecules, there may be interchanges between kinetic and internal (i.e., vibrational and rotational) energies. Such interchanges are not taken into account in the Chapman–Enskog theory for monatomic gases. At this stage, it was anticipated that the Chapman–Enskog theory would not be adequate for describing the thermal conductivity of polyatomic molecules.[16]

Huber et al.[10] have proposed a method for predicting thermal conductivity of pure refrigerants. Based on this method, the thermal conductivity of a pure fluid necessitates a summation of two parts:

$$\lambda(\rho, T) = \lambda'(\rho, T) + \lambda''(T), \tag{19}$$

where $\lambda'$ represents the translational contribution due to purely collisional effects and $\lambda''$ is the transfer of energy from internal (rotational and vibrational) contributions. It is also assumed that the transfer of energy associated with internal degrees of freedom, $\lambda''$, is independent of density and for the case of pure fluids can be calculated from the modified Eucken correlation for polyatomic gases:

$$\lambda''(T) = \frac{f_{\mathrm{int}} \eta^*(T)}{M} \left[ C_p^0(T) - \frac{5}{2} R \right], \tag{20}$$

where $\eta^*$ is the dilute gas viscosity, $M$ is the molar mass of the compound, $C_p^0$ is the constant pressure heat capacity of an ideal gas, and $f_{\mathrm{int}}$ is a constant equal to $1.32 \times 10^3$. The units for $R$ and $C_p$ are in $\mathrm{J\,mol^{-1}\,K^{-1}}$, $\eta$ in mPa s, and for $\lambda$ is in $\mathrm{W\,m^{-1}\,K^{-1}}$.

The translational term $\lambda'$ in Eq. 19 is expressed as the sum of a low-density contribution, $\lambda^*$, and a density-dependent contribution, $\lambda^+$, as follows:

$$\lambda'(\rho, T) = \lambda^*(T) + \lambda^+(\rho, T). \tag{21}$$

The low-density contribution is determined with the following formula:

$$\lambda^*(T) = \frac{15R\eta^*(T)}{4M}. \tag{22}$$

Recently, Huber and his co-workers[11] have modified their method by using $f_{\mathrm{int}}$ as a simple temperature-dependent function. In the present study, not only did we adopt their new method, but also, compared the results with those calculated from their previous scheme.[10]

## Determining Pair Potential Energy from the Viscosity Data

Boushehri[17] has proposed a direct method for determining the potential energy from transport coefficient data in the form of law of corresponding states. This method has been further elaborated by Papari and his co-workers. They have applied it to non-polar polyatomic gases,[5,6] and some binary gas mixtures of noble gases and nonpolar polyatomic molecules.[7,18,19] The novelty of the previous[4] and present work is the use of the inversion method with refrigerants which are rather polar molecules.

Monchick[20] has clarified why the inversion method works. He has shown that the Eikonal approximation to the viscosity can be inverted for certain classes of potential despite three layers of averaging. Moreover, Trusler[21] has provided the physical reasoning why an inversion of transport collision integrals, i.e. he has pointed out that most of the features implicit to the inversion method could be understood in terms of a simple perturbation treatment.

The inversion method relies on the Chapman–Enskog rigorous kinetic theory of gases which is a well developed for spherical interactions. The iterative method converges rapidly when a suitable initial potential is chosen to start the iteration. This method has been explained elsewhere,[5] and in the interest of brevity, only a breif description will be given here. Given a set of experimental viscosity data over a wide range of temperatures, with an initial model potential, such as LJ (12–6), it is possible to invert a pair of values $(\Omega^{*(2,2)}, T^*)$ to $u/\varepsilon$ as a function of $r/\sigma$ using the relations:

$$\frac{u}{\varepsilon} = u^* = GT^*, \tag{23}$$

and

$$\frac{r}{\sigma} = r^* = \left(\Omega^{*(2,2)}\right)^{1/2}. \tag{24}$$

By virtue of Eqs. 4 and 6. The inversion function $G$ is a sole function of the reduced temperature $T^*$ in a complicated way and can be calculated using a known model for intermolecular potential energy. Accordingly, the values of G for the LJ(12–6) model potential, used as the initial model, have been determined by Viehland et al.[22] The new potential energies are closer approximations to the true potential than to the initial potential energies. The new potential can be employed to calculate improved collision integrals using the sequence of Eqs. 1–3. The convergence condition stipulates the degree to which the calculated collision integrals for a given iteration are close to the experimental ones within a pre-set experimental accuracy. It should be mentioned that the rate of convergence of iteration reflects the differences between the initial potential and the potential obtained around an iteration. Of course, the closer the two potential functions are, the faster the convergence is. Interestingly, the values converged after two iterations.

## Results and Discussion

In this study, a detailed iterative inversion technique was implemented to define the intermolecular pair interaction potential energies of refrigerants from corresponding states of viscosity. Within this framework, usage of the inverted pair potential energies coupled with the Chapman–Enskog version of the kinetic theory of gases[12] was crucial in predicting the viscosity, diffusion, and thermal diffusion factor. On the other hand, the method recommended by Huber et al.[10,11] for predicting the thermal conductivity of pure refrigerants was also applied, resulting in reasonable accuracies.

To implement the full inversion procedure, the experimental data should be extended over the widest possible temperature range. In this respect, we gathered the experimental reduced viscosity collision integrals ($\Omega^{*(2,2)}$) obtained from the extended corresponding states correlations from the reported data[15,23,24] and performed a direct data inversion to determine the reduced potential energy curves.

In order to establish the intermolecular pair potential energies of methane, ethane, propane, and butane gases using the inversion procedure, the reduced viscosity collision integrals, $\Omega^{*(2,2)}$, were taken from Boushehri et al.[15] for pure methane and ethane and from Najafi et al.[23] for pure propane and butane systems. For the remaining refrigerants, values of $\Omega^{*(2,2)}$ were taken from Neufeld et al.[24] In each case, a two-iterative inversion procedure, outlined in previous section, was applied to the reduced viscosity collision integrals to generate isotropoic and effective pair potential energies of respective systems. To yield the potential energy, inversion of the viscosity collision integrals requires experimental data over an extended range of temperatures. The reduced viscosity collision integrals for methane and ethane,[15] propane and butane,[23] and R22, R32, R123, R124, R134a, R143a, and R152a[24] are related to the temperature as follows: $T^* \geq 1$, $T^* \geq 0.8$, and $0.3 \leq T^* \leq 100$, respectively. Consequently, in order to integrate Eqs. 1–3, over the given ranges, $u(r)$ should be extrapolated in the long-range region (meaning low temperature). The long-range part of $u(r)$ has the form:

$$u(r) = -\frac{C_6}{r^6} - \frac{C_8}{r^8} - \frac{C_{10}}{r^{10}} \cdots . \tag{25}$$

Note that the effects of $C_8$ and $C_{10}$ on the transport properties were so small that enabled us to neglect them in our calculations. The value of $C_6$ was estimated from the low-temperature viscosity data. Therefore, the effective potential energies obtained from the inversion method were integrated over the whole range. In turn, this permitted us to evaluate the improved kinetic theory collision integrals. Results for the most commonly needed collision integrals and their ratios obtained from Eqs. 10–14 together with Eq. 18 are given in Tables 1–3.

The remarkable benefit of the ratios of collision integrals obtained from the inversion of the vicosity collision integrals is that their accuracies are expected to be higher than those obtained from other corresponding state correlations because the measurements of the viscosity are more practical and accurate than the measurements of other transport properties, such as diffusion and thermal conductivity. Generally, calculations of the other properties are performed using numerical tables of collision integrals and their ratios.

It was found that the results after a certain number of iterations were insensitive to the variation of both the initial approximation of the potential energy and the extrapolations employed. This shows that the initial potential is a reasonable guess of the true value. In addition, the results obtained after three iterations were identical to those obtained after two iterations.

To assess the performance of the present model, viscosity, diffusion, and isotopic thermal diffusion factor were calculated and compared with reliable data published in the literature. In the present work, the known accurate values of the viscosity were used to predict other properties of which the values from experimental observations are known to be less precise. The viscosity is usually measured with greater accuracies than the diffusion coefficients and thermal diffusion factors. By employing $u(r)$, we used the accurate viscosity to improve other transport properties, i.e., the diffusion coefficients. In this respect, the transport properties of the refrigerants were determined from the recommended potential energies.

In order to calculate transport properties, we needed to know the scaling parameters $\sigma$ and $\varepsilon$ for each case. For methane and ethane systems, we took these values from Boushehri et al.[15] The values for propane and butane were reported by

Table 1. Reduced Collision Integrals and Their Ratios for Pure Methane and Ethane Systems

| $\log T^*$ | $\Omega^{*(1,1)}$ | $A^*$ | $B^*$ | $C^*$ | $E^*$ | $F^*$ | $H^*$ |
|---|---|---|---|---|---|---|---|
| 0.0 | 1.4066 | 1.1082 | 1.2013 | 0.8499 | 0.8834 | 0.9210 | −0.4698 |
| 0.1 | 1.2719 | 1.1038 | 1.1730 | 0.8593 | 0.8901 | 0.9276 | −0.4827 |
| 0.2 | 1.1589 | 1.0998 | 1.1481 | 0.8719 | 0.9006 | 0.9369 | −0.3211 |
| 0.3 | 1.0658 | 1.0974 | 1.1290 | 0.8858 | 0.9128 | 0.9478 | −0.1531 |
| 0.4 | 0.9896 | 1.0969 | 1.1153 | 0.8993 | 0.9249 | 0.9593 | −0.0210 |
| 0.5 | 0.9270 | 1.0983 | 1.1068 | 0.9112 | 0.9356 | 0.9703 | 0.0805 |
| 0.6 | 0.8748 | 1.1012 | 1.1020 | 0.9209 | 0.9441 | 0.9803 | 0.1549 |
| 0.7 | 0.8306 | 1.1051 | 1.0997 | 0.9285 | 0.9504 | 0.9891 | 0.2103 |
| 0.8 | 0.7921 | 1.1094 | 1.0987 | 0.9340 | 0.9547 | 0.9964 | 0.2485 |
| 0.9 | 0.7579 | 1.1137 | 1.0985 | 0.9379 | 0.9575 | 1.0024 | 0.2756 |
| 1.0 | 0.7268 | 1.1177 | 1.0988 | 0.9406 | 0.9592 | 1.0071 | 0.2952 |
| 1.1 | 0.6980 | 1.1216 | 1.1003 | 0.9423 | 0.9606 | 1.0104 | 0.3131 |
| 1.2 | 0.6710 | 1.1259 | 1.1037 | 0.9430 | 0.9618 | 1.0126 | 0.3330 |
| 1.3 | 0.6450 | 1.1312 | 1.1089 | 0.9426 | 0.9625 | 1.0142 | 0.3543 |
| 1.4 | 0.6196 | 1.1372 | 1.1139 | 0.9413 | 0.9615 | 1.0164 | 0.3697 |
| 1.5 | 0.5947 | 1.1422 | 1.1148 | 0.9398 | 0.9583 | 1.0200 | 0.3651 |
| 1.6 | 0.5703 | 1.1434 | 1.1084 | 0.9393 | 0.9531 | 1.0248 | 0.3319 |
| 1.7 | 0.5472 | 1.1387 | 1.0942 | 0.9410 | 0.9479 | 1.0294 | 0.2765 |
| 1.8 | 0.5260 | 1.1270 | 1.0742 | 0.9456 | 0.9448 | 1.0323 | 0.2170 |
| 1.9 | 0.5078 | 1.1095 | 1.0522 | 0.9527 | 0.9453 | 1.0324 | 0.1715 |
| 2.0 | 0.4930 | 1.0887 | 1.0316 | 0.9616 | 0.9498 | 1.0301 | 0.1486 |

Table 2. Reduced Collision Integrals and Their Ratios for Pure Propane and Butane Systems

| $\log T^*$ | $\Omega^{*(1,1)}$ | $A^*$ | $B^*$ | $C^*$ | $E^*$ | $F^*$ | $H^*$ |
|---|---|---|---|---|---|---|---|
| −0.1 | 1.5297 | 1.1105 | 1.2189 | 0.8448 | 0.8842 | 0.9174 | −0.3561 |
| 0.0 | 1.3770 | 1.1098 | 1.1958 | 0.8512 | 0.8865 | 0.9223 | −0.5168 |
| 0.1 | 1.2464 | 1.1073 | 1.1719 | 0.8610 | 0.8928 | 0.9296 | −0.4114 |
| 0.2 | 1.1368 | 1.1046 | 1.1497 | 0.8731 | 0.9025 | 0.9390 | −0.2611 |
| 0.3 | 1.0140 | 1.1030 | 1.1318 | 0.8862 | 0.9139 | 0.9502 | −0.1179 |
| 0.4 | 0.9713 | 1.1031 | 1.1188 | 0.8989 | 0.9250 | 0.9619 | −0.0005 |
| 0.5 | 0.9094 | 1.1049 | 1.1103 | 0.9103 | 0.9351 | 0.9732 | 0.0925 |
| 0.6 | 0.8576 | 1.1079 | 1.1056 | 0.9196 | 0.9432 | 0.9830 | 0.1631 |
| 0.7 | 0.8133 | 1.1119 | 1.1038 | 0.9268 | 0.9494 | 0.9914 | 0.2179 |
| 0.8 | 0.7747 | 1.1166 | 1.1039 | 0.9319 | 0.9537 | 0.9982 | 0.2589 |
| 0.9 | 0.7400 | 1.1216 | 1.1053 | 0.9354 | 0.9564 | 1.0037 | 0.2911 |
| 1.0 | 0.7082 | 1.1268 | 1.1077 | 0.9374 | 0.9581 | 1.0079 | 0.3163 |
| 1.1 | 0.6784 | 1.1323 | 1.1114 | 0.9381 | 0.9591 | 1.0110 | 0.3385 |
| 1.2 | 0.6500 | 1.1386 | 1.1172 | 0.9377 | 0.9599 | 1.0131 | 0.3638 |
| 1.3 | 0.6223 | 1.1461 | 1.1246 | 0.9362 | 0.9598 | 1.0147 | 0.3905 |
| 1.4 | 0.5950 | 1.1546 | 1.1321 | 0.9336 | 0.9582 | 1.0168 | 0.4121 |
| 1.5 | 0.5677 | 1.1626 | 1.1368 | 0.9307 | 0.9545 | 1.0198 | 0.4187 |
| 1.6 | 0.5407 | 1.1676 | 1.1353 | 0.9283 | 0.9488 | 1.0240 | 0.3961 |
| 1.7 | 0.5144 | 1.1673 | 1.1256 | 0.9278 | 0.9423 | 1.0287 | 0.3416 |
| 1.8 | 0.4897 | 1.1596 | 1.1074 | 0.9301 | 0.9368 | 1.0328 | 0.2632 |
| 1.9 | 0.4674 | 1.1444 | 1.0835 | 0.9359 | 0.9343 | 1.0350 | 0.1883 |
| 2.0 | 0.4485 | 1.1232 | 1.0578 | 0.9448 | 0.9361 | 1.0346 | 0.1379 |

Najafi et al.[23] In the case of R134a, R123, and R152a, the values of $\varepsilon$ and $\sigma$ were reported by Nabizadeh and Mayinger[25] and by Krauss et al.,[26] respectivley. Lastly, for the four remaining refrigerants R22, R32, R143a, and R124, we calculated the values of $\sigma$ using the following equation:

$$\sigma = 0.809(V_c)^{1/3}, \tag{26}$$

where $V_c$ is critical volume and the values of $\varepsilon$ were calculated using a corresponding states correlation for $\Omega^{*(2,2)}$ using a non-linear least squares method, reported by Rigby et al.[27]

Expressions provided by the Chapman–Enskog version of the kinetic theory, Chapman and Cowling[12] and Hirschfelder et al.,[13] together with the calculated collision integrals obtained from the inverted potential energies, were employed

Table 3. Reduced Collision Integrals and Their Ratios for Other Pure Refrigerant Systems

| $\log T^*$ | $\Omega^{*(1,1)}$ | $A^*$ | $B^*$ | $C^*$ | $E^*$ | $F^*$ | $H^*$ |
|---|---|---|---|---|---|---|---|
| −0.5 | 2.5802 | 1.0771 | 1.2893 | 0.8470 | 0.9036 | 0.9003 | 2.4378 |
| −0.4 | 2.3117 | 1.0938 | 1.2958 | 0.8511 | 0.8909 | 0.8962 | 2.2889 |
| −0.3 | 2.0559 | 1.1055 | 1.2844 | 0.8263 | 0.8780 | 0.8947 | −1.4455 |
| −0.2 | 1.8207 | 1.1106 | 1.2588 | 0.8231 | 0.8692 | 0.8962 | 0.5700 |
| −0.1 | 1.6128 | 1.1099 | 1.2256 | 0.8269 | 0.8672 | 0.9008 | 2.8964 |
| 0.0 | 1.4354 | 1.1055 | 1.1914 | 0.8369 | 0.8724 | 0.9086 | −7.2149 |
| 0.1 | 1.2887 | 1.0999 | 1.1609 | 0.8515 | 0.8832 | 0.9193 | −1.4523 |
| 0.2 | 1.1698 | 1.0951 | 1.1366 | 0.8684 | 0.8973 | 0.9318 | −0.6169 |
| 0.3 | 1.0744 | 1.0922 | 1.1189 | 0.8853 | 0.9122 | 0.9451 | −0.2614 |
| 0.4 | 0.9979 | 1.0915 | 1.1071 | 0.9007 | 0.9259 | 0.9582 | −0.0606 |
| 0.5 | 0.9361 | 1.0929 | 1.0998 | 0.9137 | 0.9374 | 0.9701 | 0.0655 |
| 0.6 | 0.8851 | 1.0956 | 1.0958 | 0.9240 | 0.9462 | 0.9805 | 0.1496 |
| 0.7 | 0.8422 | 1.0993 | 1.0938 | 0.9318 | 0.9527 | 0.9892 | 0.2068 |
| 0.8 | 0.8050 | 1.1033 | 1.0930 | 0.9374 | 0.9570 | 0.9964 | 0.2457 |
| 0.9 | 0.7721 | 1.1073 | 1.0928 | 0.9414 | 0.9598 | 1.0023 | 0.2727 |
| 1.0 | 0.7422 | 1.1109 | 1.0924 | 0.9441 | 0.9612 | 1.0072 | 0.2886 |
| 1.1 | 0.7146 | 1.1136 | 1.0906 | 0.9462 | 0.9614 | 1.0116 | 0.2939 |
| 1.2 | 0.6890 | 1.1142 | 1.0859 | 0.9482 | 0.9604 | 1.0161 | 0.2857 |
| 1.3 | 0.6653 | 1.1115 | 1.0770 | 0.9509 | 0.9586 | 1.0204 | 0.2642 |
| 1.4 | 0.6440 | 1.1046 | 1.0641 | 0.9548 | 0.9570 | 1.0240 | 0.2348 |
| 1.5 | 0.6253 | 1.0933 | 1.0486 | 0.9602 | 0.9502 | 1.0260 | 0.2062 |
| 1.6 | 0.6097 | 1.0787 | 1.0328 | 0.9668 | 0.9593 | 1.0259 | 0.1863 |
| 1.7 | 0.5973 | 1.0626 | 1.0188 | 0.9739 | 0.9639 | 1.0240 | 0.1776 |
| 1.8 | 0.5881 | 1.0470 | 1.0077 | 0.9810 | 0.9703 | 1.0208 | 0.1796 |
| 1.9 | 0.5817 | 1.0332 | 0.9998 | 0.9873 | 0.9773 | 1.0172 | 0.1875 |
| 2.0 | 0.5777 | 1.0221 | 0.9950 | 0.9925 | 0.9840 | 1.0139 | 0.1989 |

Table 4. Predicted Transport Properties of Pure Methane System

| $T$/K | $10^6\ \eta$/Pa s | $10^4$ D/m$^2$ s$^{-1}$ | $\alpha_0$ | $10^3\ \lambda$/W m$^{-1}$ K$^{-1}$ |
|---|---|---|---|---|
| 200 | 7.715 | 0.1046 | 0.1263 | 22.758 |
| 250 | 9.479 | 0.1601 | 0.1858 | 28.826 |
| 273.15 | 10.242 | 0.1888 | 0.2110 | 31.764 |
| 293.15 | 10.889 | 0.2153 | 0.2321 | 34.425 |
| 300 | 11.116 | 0.2249 | 0.2393 | 35.387 |
| 313.15 | 11.559 | 0.2440 | 0.2532 | 37.311 |
| 333.15 | 12.186 | 0.2735 | 0.2718 | 40.217 |
| 353.15 | 12.772 | 0.3039 | 0.2882 | 43.140 |
| 373.15 | 13.368 | 0.3361 | 0.3047 | 46.255 |
| 423.15 | 14.827 | 0.4227 | 0.3416 | 54.589 |
| 473.15 | 16.171 | 0.5157 | 0.3707 | 63.386 |
| 523.15 | 17.503 | 0.6176 | 0.3973 | 72.934 |
| 573.15 | 18.710 | 0.7240 | 0.4163 | 82.637 |
| 623.15 | 19.933 | 0.8394 | 0.4352 | 92.967 |
| 673.15 | 21.080 | 0.9599 | 0.4498 | 103.390 |
| 723.15 | 22.172 | 1.0858 | 0.4615 | 113.870 |
| 773.15 | 23.270 | 1.2196 | 0.4733 | 124.620 |
| 873.15 | 25.333 | 1.5024 | 0.4902 | 145.880 |
| 973.15 | 27.316 | 1.8089 | 0.5035 | 167.210 |

to calculate viscosities and self-diffusion coefficients of the aforementioned gases. Tables 4–14 contain a brief listing of the transport properties of the eleven gases studied at selected temperatures that lie within $200\,\mathrm{K} < T < 1000\,\mathrm{K}$. The calculated viscosities were correlated with the following equation:

$$\ln\left(\frac{\eta}{\eta_0}\right) = a_\eta \ln\left(\frac{T}{T_0}\right) + \frac{b_\eta}{T} + \frac{c_\eta}{T^2} + d_\eta, \tag{27}$$

where $\eta_0 = 1\ \mu$ Pa s and $T_0 = 1\,\mathrm{K}$. Parameters in the above equation were allowed to vary for all the systems using nonlinear least-squares method and are listed in Table 15. The cor-

Table 5. Predicted Transport Properties of Pure Ethane System

| $T$/K | $10^6\ \eta$/Pa s | $10^4$ D/m$^2$ s$^{-1}$ | $\alpha_0$ | $10^3\ \lambda$/W m$^{-1}$ K$^{-1}$ |
|---|---|---|---|---|
| 200 | 6.518 | 0.0474 | 0.0517 | 12.589 |
| 250 | 7.874 | 0.0714 | 0.0892 | 17.264 |
| 273.15 | 8.549 | 0.0846 | 0.1064 | 19.705 |
| 293.15 | 9.163 | 0.0972 | 0.1214 | 22.049 |
| 300 | 9.380 | 0.1018 | 0.1265 | 22.905 |
| 313.15 | 9.759 | 0.1104 | 0.1367 | 24.503 |
| 333.15 | 10.310 | 0.1240 | 0.1526 | 26.991 |
| 353.15 | 10.879 | 0.1386 | 0.1686 | 29.667 |
| 373.15 | 11.468 | 0.1542 | 0.1845 | 32.540 |
| 423.15 | 12.799 | 0.1949 | 0.2207 | 39.886 |
| 473.15 | 14.147 | 0.2407 | 0.2559 | 48.002 |
| 523.15 | 15.367 | 0.2889 | 0.2848 | 56.275 |
| 573.15 | 16.580 | 0.3415 | 0.3123 | 64.967 |
| 623.15 | 17.774 | 0.3980 | 0.3374 | 73.920 |
| 673.15 | 18.854 | 0.4562 | 0.3567 | 82.612 |
| 723.15 | 19.953 | 0.5189 | 0.3762 | 91.512 |
| 773.15 | 21.049 | 0.5854 | 0.3946 | 100.460 |
| 873.15 | 23.006 | 0.7236 | 0.4198 | 117.430 |
| 973.15 | 24.975 | 0.8767 | 0.4442 | 135.100 |

Table 6. Predicted Transport Properties of Pure Propane System

| $T$/K | $10^6\ \eta$/Pa s | $10^4$ D/m$^2$ s$^{-1}$ | $\alpha_0$ | $10^3\ \lambda$/W m$^{-1}$ K$^{-1}$ |
|---|---|---|---|---|
| 250 | 7.103 | 0.0440 | 0.0444 | 14.343 |
| 273.15 | 7.660 | 0.0519 | 0.0545 | 16.464 |
| 293.15 | 8.158 | 0.0593 | 0.0632 | 18.468 |
| 300 | 8.333 | 0.0620 | 0.0662 | 19.194 |
| 313.15 | 8.676 | 0.0673 | 0.0719 | 20.644 |
| 333.15 | 9.216 | 0.0761 | 0.0805 | 23.002 |
| 353.15 | 9.780 | 0.0856 | 0.0891 | 25.553 |
| 373.15 | 10.272 | 0.0949 | 0.0997 | 28.037 |
| 423.15 | 11.564 | 0.1211 | 0.1263 | 34.906 |
| 473.15 | 12.825 | 0.1500 | 0.1525 | 42.306 |
| 523.15 | 14.051 | 0.1815 | 0.1786 | 50.100 |
| 573.15 | 15.289 | 0.2167 | 0.2038 | 58.350 |
| 623.15 | 16.408 | 0.2553 | 0.2264 | 66.436 |
| 673.15 | 17.567 | 0.2984 | 0.2490 | 74.870 |
| 723.15 | 18.699 | 0.3426 | 0.2698 | 83.315 |
| 773.15 | 19.728 | 0.3833 | 0.2874 | 91.365 |
| 873.15 | 21.855 | 0.4713 | 0.3227 | 107.950 |
| 973.15 | 23.775 | 0.5703 | 0.3494 | 124.130 |

Table 7. Predicted Transport Properties of Pure Butane System

| $T$/K | $10^6\ \eta$/Pa s | $10^4$ D/m$^2$ s$^{-1}$ | $\alpha_0$ | $10^3\ \lambda$/W m$^{-1}$ K$^{-1}$ |
|---|---|---|---|---|
| 273.15 | 7.300 | 0.0375 | 0.0236 | 15.834 |
| 293.15 | 7.706 | 0.0425 | 0.0301 | 17.571 |
| 300 | 7.846 | 0.0443 | 0.0327 | 18.192 |
| 313.15 | 8.117 | 0.0478 | 0.0367 | 19.425 |
| 333.15 | 8.537 | 0.0535 | 0.0432 | 21.399 |
| 353.15 | 8.965 | 0.0596 | 0.0497 | 23.493 |
| 373.15 | 9.404 | 0.0660 | 0.0561 | 25.714 |
| 423.15 | 10.553 | 0.0840 | 0.0725 | 31.830 |
| 473.15 | 11.795 | 0.1049 | 0.0883 | 38.793 |
| 523.15 | 12.921 | 0.1270 | 0.1077 | 45.859 |
| 573.15 | 14.101 | 0.1517 | 0.1275 | 53.478 |
| 623.15 | 15.250 | 0.1782 | 0.1473 | 61.265 |
| 673.15 | 16.334 | 0.2060 | 0.1667 | 68.983 |
| 723.15 | 17.462 | 0.2365 | 0.1861 | 77.001 |
| 773.15 | 18.562 | 0.2693 | 0.2041 | 84.977 |
| 873.15 | 20.596 | 0.3425 | 0.2381 | 100.360 |
| 973.15 | 22.657 | 0.4239 | 0.2698 | 116.490 |

Table 8. Predicted Transport Properties of Pure R134a System

| $T$/K | $10^6\ \eta$/Pa s | $10^4$ D/m$^2$ s$^{-1}$ | $\alpha_0$ | $10^3\ \lambda$/W m$^{-1}$ K$^{-1}$ |
|---|---|---|---|---|
| 200 | 7.731 | 0.0166 | −0.0430 | 7.055 |
| 250 | 9.722 | 0.0260 | −0.0140 | 10.114 |
| 273.15 | 10.668 | 0.0311 | 0.0078 | 11.705 |
| 293.15 | 11.461 | 0.0358 | 0.0282 | 13.124 |
| 300 | 11.713 | 0.0374 | 0.0350 | 13.601 |
| 313.15 | 12.207 | 0.0407 | 0.0480 | 14.547 |
| 333.15 | 12.987 | 0.0460 | 0.0678 | 16.065 |
| 353.15 | 13.805 | 0.0518 | 0.0876 | 17.684 |
| 373.15 | 14.520 | 0.0575 | 0.1060 | 19.217 |
| 423.15 | 16.333 | 0.0732 | 0.1516 | 23.244 |
| 473.15 | 18.105 | 0.0905 | 0.1928 | 27.395 |
| 523.15 | 19.772 | 0.1092 | 0.2295 | 31.500 |
| 573.15 | 21.472 | 0.1298 | 0.2648 | 35.716 |
| 623.15 | 22.963 | 0.1508 | 0.2917 | 39.590 |
| 673.15 | 24.495 | 0.1738 | 0.3187 | 43.500 |
| 723.15 | 26.011 | 0.1982 | 0.3436 | 47.332 |
| 773.15 | 27.358 | 0.2230 | 0.3619 | 50.794 |
| 873.15 | 30.110 | 0.2773 | 0.3985 | 57.697 |
| 973.15 | 32.621 | 0.3351 | 0.4246 | 64.245 |

relation coefficients ($R$), and standard errors (SE), for each case have also been included.

Figure 1 shows a comparison of our calculated viscosities for methane with the literature data.[28–37] The possibility of pyrolysis of pure methane at high temperatures caused us to limit the temperature range over which its transport properties were calculated. In the present work, the viscosity of methane was calculated in temperature range between 200 and 1000 K.

The viscosities of the dilute ethane gas are compared with experimental measurements[28,33,36–41] in Fig. 2. Figure 3 illustrates the deviations of the predicted viscosities for propane from the experimental observations.[28,30,32,33,36,37,42,43] Obviously, the predicted viscosities are in very good agreement with those reported by Abe et al.[28] and Kestin et al.,[36] in the temperature interval of 300 K $< T <$ 500 K.

It is known that $n$-butane is a component of natural gas and is an environmentally friendly alternative refrigerant. Therefore, its thermophysical properties must be determined in the widest range of temperatures possible. A deviation plot is displayed in Fig. 4 for the calculated viscosities of $n$-butane along with the literature values.[28–30,33,36,37,44,45]

The collective comparisons in Figs. 1–4 with literature values show good agreement in all cases. In general, the accuracies were within a band of 2% in the temperature range 200 K $< T <$ 1000 K.

Shown in Figs. 5–10 is a comparison of the calculated vis-

Table 9. Predicted Transport Properties of Pure R152a System

| $T$/K | $10^6\ \eta$/Pa s | $10^4$ D/m$^2$ s$^{-1}$ | $\alpha_0$ | $10^3\ \lambda$/W m$^{-1}$ K$^{-1}$ |
|---|---|---|---|---|
| 200 | 6.704 | 0.0221 | −0.0440 | 7.548 |
| 250 | 8.412 | 0.0348 | −0.0430 | 10.751 |
| 273.15 | 9.240 | 0.0418 | −0.0350 | 12.464 |
| 293.15 | 9.933 | 0.0482 | −0.0240 | 14.006 |
| 300 | 10.159 | 0.0504 | −0.0200 | 14.537 |
| 313.15 | 10.602 | 0.0548 | −0.0110 | 15.594 |
| 333.15 | 11.304 | 0.0621 | 0.0033 | 17.308 |
| 353.15 | 12.046 | 0.0701 | 0.0170 | 19.162 |
| 373.15 | 12.689 | 0.0780 | 0.0327 | 20.930 |
| 423.15 | 14.366 | 0.0998 | 0.0721 | 25.740 |
| 473.15 | 16.010 | 0.1241 | 0.1099 | 30.834 |
| 523.15 | 17.586 | 0.1505 | 0.1462 | 36.062 |
| 573.15 | 19.196 | 0.1796 | 0.1810 | 41.555 |
| 623.15 | 20.620 | 0.2096 | 0.2103 | 46.766 |
| 673.15 | 22.098 | 0.2424 | 0.2396 | 52.156 |
| 723.15 | 23.554 | 0.2774 | 0.2667 | 57.518 |
| 773.15 | 24.851 | 0.3129 | 0.2881 | 62.479 |
| 873.15 | 27.532 | 0.3913 | 0.3313 | 72.581 |
| 973.15 | 29.951 | 0.4746 | 0.3629 | 82.183 |

Table 10. Predicted Transport Properties of Pure R123 System

| $T$/K | $10^6\ \eta$/Pa s | $10^4$ D/m$^2$ s$^{-1}$ | $\alpha_0$ | $10^3\ \lambda$/W m$^{-1}$ K$^{-1}$ |
|---|---|---|---|---|
| 200 | 7.037 | 0.0101 | −0.0410 | 5.119 |
| 250 | 8.848 | 0.0158 | −0.0070 | 7.301 |
| 273.15 | 9.720 | 0.0189 | 0.0131 | 8.429 |
| 293.15 | 10.419 | 0.0217 | 0.0324 | 9.397 |
| 300 | 10.650 | 0.0227 | 0.0393 | 9.728 |
| 313.15 | 11.104 | 0.0247 | 0.0525 | 10.380 |
| 333.15 | 11.821 | 0.0279 | 0.0726 | 11.430 |
| 353.15 | 12.561 | 0.0314 | 0.0925 | 12.530 |
| 373.15 | 13.193 | 0.0348 | 0.1109 | 13.540 |
| 423.15 | 14.857 | 0.0444 | 0.1571 | 16.230 |
| 473.15 | 16.439 | 0.0548 | 0.1977 | 18.920 |
| 523.15 | 17.967 | 0.0662 | 0.2351 | 21.590 |
| 573.15 | 19.478 | 0.0785 | 0.2692 | 24.250 |
| 623.15 | 20.841 | 0.0913 | 0.2965 | 26.710 |
| 673.15 | 22.243 | 0.1053 | 0.3239 | 29.200 |
| 723.15 | 23.582 | 0.1199 | 0.3474 | 31.570 |
| 773.15 | 24.815 | 0.1349 | 0.3659 | 33.750 |
| 873.15 | 27.324 | 0.1679 | 0.4031 | 38.070 |
| 973.15 | 29.567 | 0.2027 | 0.4278 | 42.000 |

Table 11. Predicted Transport Properties of Pure R22 System

| $T$/K | $10^6\ \eta$/Pa s | $10^4$ D/m$^2$ s$^{-1}$ | $\alpha_0$ | $10^3\ \lambda$/W m$^{-1}$ K$^{-1}$ |
|---|---|---|---|---|
| 200 | 8.334 | 0.0210 | −0.0450 | 6.206 |
| 250 | 10.463 | 0.0331 | −0.0410 | 8.605 |
| 273.15 | 11.509 | 0.0397 | −0.0330 | 9.872 |
| 293.15 | 12.339 | 0.0457 | −0.0200 | 10.950 |
| 300 | 12.623 | 0.0478 | −0.0160 | 11.340 |
| 313.15 | 13.182 | 0.0521 | −0.0060 | 12.090 |
| 333.15 | 14.070 | 0.0590 | 0.0077 | 13.310 |
| 353.15 | 14.962 | 0.0665 | 0.0223 | 14.580 |
| 373.15 | 15.756 | 0.0739 | 0.0384 | 15.790 |
| 423.15 | 17.870 | 0.0948 | 0.0786 | 19.070 |
| 473.15 | 19.865 | 0.1176 | 0.1165 | 22.390 |
| 523.15 | 21.847 | 0.1427 | 0.1535 | 25.800 |
| 573.15 | 23.786 | 0.1700 | 0.1875 | 29.220 |
| 623.15 | 25.570 | 0.1985 | 0.2174 | 32.470 |
| 673.15 | 27.426 | 0.2297 | 0.2474 | 35.810 |
| 723.15 | 29.159 | 0.2623 | 0.2727 | 38.960 |
| 773.15 | 30.780 | 0.2959 | 0.2946 | 41.910 |
| 873.15 | 34.142 | 0.3705 | 0.3386 | 47.900 |
| 973.15 | 37.063 | 0.4486 | 0.3684 | 53.380 |

Table 12. Predicted Transport Properties of Pure R143a System

| $T$/K | $10^6\ \eta$/Pa s | $10^4$ D/m$^2$ s$^{-1}$ | $\alpha_0$ | $10^3\ \lambda$/W m$^{-1}$ K$^{-1}$ |
|---|---|---|---|---|
| 200 | 8.460 | 0.0220 | −0.0380 | 8.454 |
| 250 | 10.631 | 0.0345 | 0.0017 | 12.167 |
| 273.15 | 11.671 | 0.0413 | 0.0234 | 14.115 |
| 293.15 | 12.477 | 0.0473 | 0.0443 | 15.773 |
| 300 | 12.762 | 0.0495 | 0.0514 | 16.369 |
| 313.15 | 13.322 | 0.0539 | 0.0652 | 17.553 |
| 333.15 | 14.211 | 0.0610 | 0.0861 | 19.464 |
| 353.15 | 15.001 | 0.0682 | 0.1056 | 21.305 |
| 373.15 | 15.775 | 0.0757 | 0.1248 | 23.178 |
| 423.15 | 17.825 | 0.0968 | 0.1729 | 28.256 |
| 473.15 | 19.619 | 0.1190 | 0.2120 | 33.174 |
| 523.15 | 21.489 | 0.1439 | 0.2509 | 38.385 |
| 573.15 | 23.182 | 0.1700 | 0.2818 | 43.379 |
| 623.15 | 24.838 | 0.1980 | 0.3103 | 48.340 |
| 673.15 | 26.548 | 0.2286 | 0.3389 | 53.407 |
| 723.15 | 28.017 | 0.2593 | 0.3582 | 57.960 |
| 773.15 | 29.503 | 0.2920 | 0.3775 | 62.498 |
| 873.15 | 32.441 | 0.3629 | 0.4126 | 71.423 |
| 973.15 | 35.101 | 0.4381 | 0.4371 | 79.911 |

cosities of the refrigerants R134a, R152a, R123, R22, R124, and R32 with those reported in the literature[3,25,26,33,46–51] respectively. The suitable agreement of the results confirms that our calculations using the inversion procedure are reliable, even though some discrepancies between the calculated viscisities and the correlation outputs obtained by Grebenkov et al.[47] were observed. Therefore, we can claim with confidence that the uncertainty ascribed to the calculted viscosity is not greater than 2%.

A consensus among researchers is that a method for obtaining reliable diffusion coefficients from the viscosity data would be useful. We believe that the inversion procedure allows us to do this. The diffusion coefficients of the eleven aforementioned refrigerant systems were calculated using the inverted pair potential energies. Numerical values of this property in an ample temperature range are given in Tables 4–14. These values were correlated with the following equation:

$$\ln(PD/P_0D_0) = a_D \ln(T/T_0) + b_D/T + c_D, \quad (28)$$

where $P_0 = 1$ atm, $D_0 = 1\,\mathrm{cm^2\,s^{-1}}$, and constants $a_D$, $b_D$, and $c_D$, are tabulated in Table 16. The table also contains correlation coefficients ($R$) and standard errors (SE) of the fitting. Figure 11 illustrates the property deviations for R134a, R123, and R124 with respect to those obtained by Dowdell and

Table 13. Predicted Transport Properties of Pure R124 System

| $T$/K | $10^6\ \eta$/Pa s | $10^4$ D/m$^2$ s$^{-1}$ | $\alpha_0$ | $10^3\ \lambda$/W m$^{-1}$ K$^{-1}$ |
|---|---|---|---|---|
| 200 | 7.719 | 0.0124 | −0.0400 | 5.989 |
| 250 | 9.704 | 0.0194 | −0.0050 | 8.548 |
| 273.15 | 10.669 | 0.0232 | 0.0158 | 9.902 |
| 293.15 | 11.415 | 0.0267 | 0.0358 | 11.053 |
| 300 | 11.671 | 0.0279 | 0.0428 | 11.459 |
| 313.15 | 12.172 | 0.0303 | 0.0561 | 12.264 |
| 333.15 | 12.966 | 0.0343 | 0.0764 | 13.562 |
| 353.15 | 13.752 | 0.0385 | 0.0962 | 14.898 |
| 373.15 | 14.448 | 0.0427 | 0.1149 | 16.178 |
| 423.15 | 16.287 | 0.0545 | 0.1616 | 19.632 |
| 473.15 | 17.994 | 0.0672 | 0.2018 | 23.078 |
| 523.15 | 19.678 | 0.0812 | 0.2396 | 26.563 |
| 573.15 | 21.304 | 0.0962 | 0.2828 | 29.954 |
| 623.15 | 22.803 | 0.1120 | 0.3004 | 33.056 |
| 673.15 | 24.346 | 0.1291 | 0.3282 | 36.017 |
| 723.15 | 25.788 | 0.1469 | 0.3505 | 38.526 |
| 773.15 | 27.129 | 0.1653 | 0.3692 | 40.476 |
| 873.15 | 29.890 | 0.2058 | 0.4068 | 42.837 |
| 973.15 | 32.315 | 0.2483 | 0.4305 | 41.759 |

Table 14. Predicted Transport Properties of Pure R32 System

| $T$/K | $10^6\ \eta$/Pa s | $10^4$ D/m$^2$ s$^{-1}$ | $\alpha_0$ | $10^3\ \lambda$/W m$^{-1}$ K$^{-1}$ |
|---|---|---|---|---|
| 200 | 8.709 | 0.0351 | −0.0510 | 8.726 |
| 250 | 10.613 | 0.0553 | −0.0320 | 11.398 |
| 273.15 | 11.576 | 0.0657 | −0.0140 | 12.899 |
| 293.15 | 12.460 | 0.0757 | 0.0014 | 14.336 |
| 300 | 12.776 | 0.0794 | 0.0067 | 14.871 |
| 313.15 | 13.363 | 0.0868 | 0.0169 | 15.887 |
| 333.15 | 14.163 | 0.0978 | 0.0345 | 17.406 |
| 353.15 | 14.995 | 0.1095 | 0.0523 | 19.056 |
| 373.15 | 15.865 | 0.1222 | 0.0700 | 20.812 |
| 423.15 | 17.868 | 0.1561 | 0.1124 | 25.343 |
| 473.15 | 19.895 | 0.1936 | 0.1532 | 30.201 |
| 523.15 | 21.774 | 0.2345 | 0.1906 | 35.030 |
| 573.15 | 23.597 | 0.2779 | 0.2236 | 35.728 |
| 623.15 | 25.463 | 0.3259 | 0.2568 | 44.177 |
| 673.15 | 27.084 | 0.3747 | 0.2819 | 47.614 |
| 723.15 | 28.744 | 0.4269 | 0.3061 | 50.198 |
| 773.15 | 30.453 | 0.4831 | 0.3305 | 51.858 |
| 873.15 | 33.408 | 0.5999 | 0.3661 | 48.172 |
| 973.15 | 36.429 | 0.7289 | 0.3991 | 34.703 |

Table 15. Least-Squares Coefficients, Correlation Coefficients ($R$), and Standard Errors (SE) for Eq. 27

| Refrigerant | $a_\eta$ | $b_\eta$/K | $c_\eta$/K$^2$ | $d_\eta$ | $R$ | SE |
|---|---|---|---|---|---|---|
| Methane | 0.57044977 | −116.47942 | 4211.4528 | −0.5028024 | 0.9999974 | 0.0145990 |
| Ethane | 0.51480732 | −235.84942 | 16911.854 | −0.1010373 | 0.99998998 | 0.0271054 |
| Propane | 0.53610688 | −296.73559 | 26709.837 | −0.2428308 | 0.99999255 | 0.0223617 |
| Butane | 0.52838104 | −411.73273 | 50698.012 | −0.1463039 | 0.9999911 | 0.0229397 |
| R134a | 0.53110237 | −232.02852 | 13459.435 | 0.0554141 | 0.9999948 | 0.0262807 |
| R152a | 0.55016026 | −270.29982 | 18726.261 | −0.1268088 | 0.9999931 | 0.0283692 |
| R123 | 0.53282077 | −227.62514 | 13005.667 | −0.0584460 | 0.9999949 | 0.0235981 |
| R22 | 0.54961858 | −266.57517 | 18247.529 | 0.08714858 | 0.9999916 | 0.0386997 |
| R143a | 0.52479996 | −225.48006 | 12650.247 | 0.16600102 | 0.9999920 | 0.0349272 |
| R124 | 0.53220688 | −226.02183 | 12849.959 | 0.03334672 | 0.9999938 | 0.0284234 |
| R32 | 0.48859487 | −305.60576 | 2398.626 | 0.52183504 | 0.9999881 | 0.0446050 |

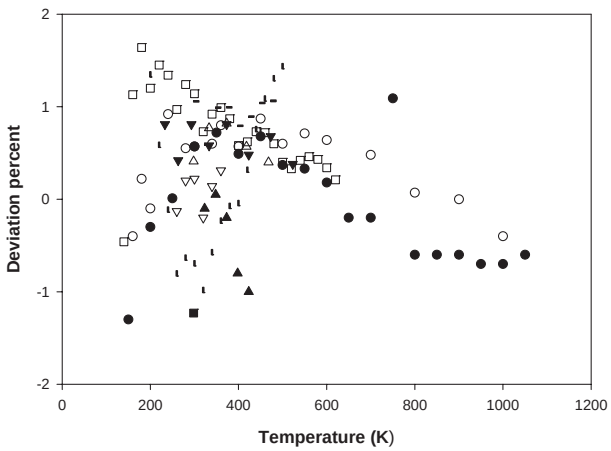


Fig. 1. Deviation plot for the viscosity coefficients of methane gaseous system at different temperatures compared with experiment: Abe et al.[28] (△), Vargaftik et al.[29] (○), Smith et al.[30] (▲), Trengove and Wakeham[31] (●), Hurly et al.[32] (■), Lemmon et al.[33] (□), Evers et al.[34] (▼), Schley et al.[35] (▽), Kestin et al.[36] (▬), Heckenberger and Stephan[37] (▮).

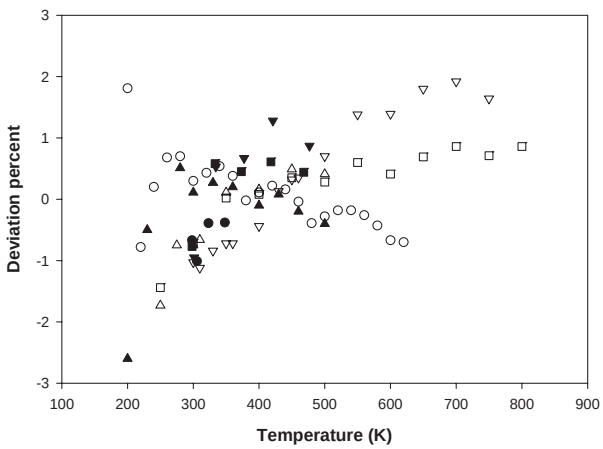


Fig. 2. Deviation plot for the viscosity coefficients of ethane gaseous system at different temperatures compared with experiment: Abe et al.[28] (■), Lemmon et al.[33] (○), Kestin et al.[36] (▼), Heckenberger and Stephan[37] (▽), Iwasaki and Takahashi[38] (●), Friend et al.[39] (▲), Hendle et al.[40] (△), Hendle et al.[41] (□).

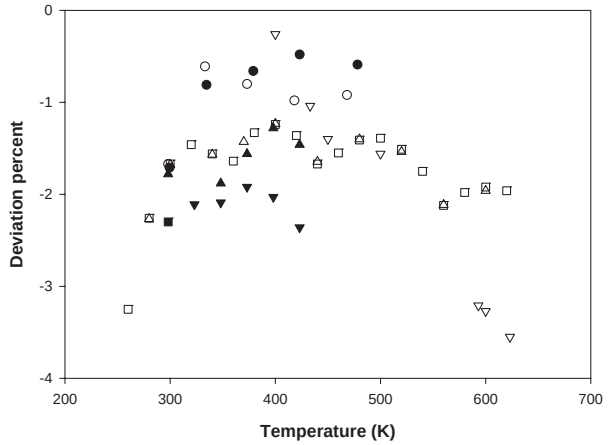


Fig. 3. Deviation plot for the viscosity coefficients of propane gaseous system at different temperatures compared with experiment: Abe et al.[28] (○), Smith et al.[30] (▼), Hurly et al.[32] (■), Lemmon et al.[33] (□), Kestin et al.[36] (●), Heckenberger and Stephan[37] (▽), Wilhelm and Vogel[42] (▲), Vogel et al.[43] (△).

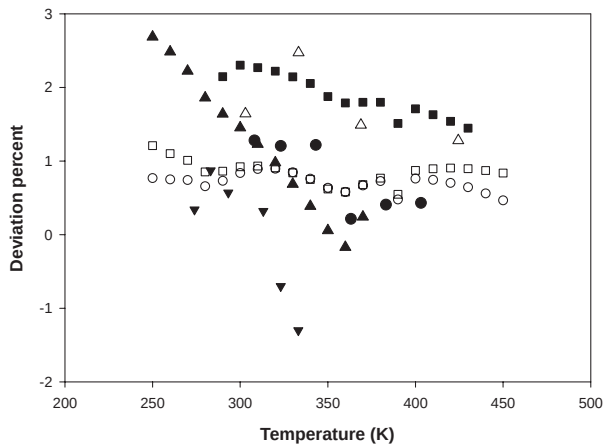


Fig. 5. Deviation plot for the viscosity coefficients of R134a gaseous system at different temperatures compared with experiment: Comuñas et al.[2] (○), Nabizadeh and Mayinger[25] (△), Lemmon et al.[33] (□), Dowdell and Matthews[46] (●), Grebenkov et al.[47] (▲), Millat et al.[48] (■), Assael and Polimatidou[49] (▼).

Matthews.[46] Basically our estimated accuracies of self-diffusion coefficients were within a 4% error band.

Isotopic thermal diffusion factors for all refrigerants were calculated using Eqs. 16–18. Results of the computations are summerized sequentially in Tables 4–14. Table 17 contains the constants of the following fourth order polynomial equation, which was fitted to the values of isotopic thermal diffusion factors, using a non-linear least-squares method. Also, the table contains correlation coefficient ($R$) and standard error (SE) of the fitting.

$$\alpha_0 = a_\alpha + b_\alpha T + C_\alpha T^2 + d_\alpha T^3 + e_\alpha T^4. \quad (29)$$

In the case of thermal conductivity, the predicted viscosities obtained via the inverted pair potential energies were employed to predict thermal conductivities in the temperature

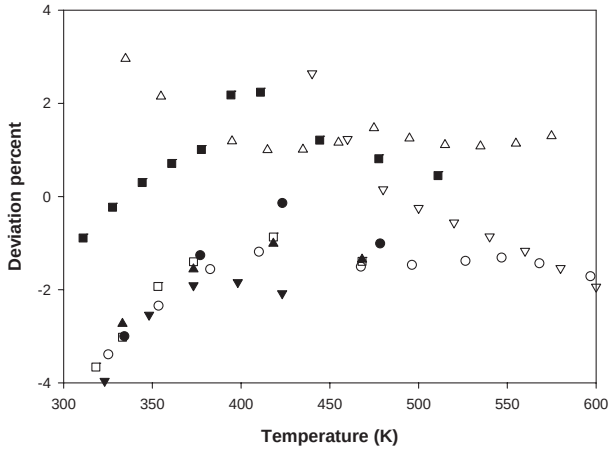


Fig. 4. Deviation plot for the viscosity coefficients of *n*-butane gaseous system at different temperatures compared with experiment: Abe et al.[28] (▲), Vargaftik et al.[29] (■), Smith et al.[30] (▼), Lemmon et al.[33] (△), Kestin et al.[36] (●), Heckenberger and Stephan[37] (▽), Kuchenmeister and Vogel[44] (○), Abe et al.[45] (□).

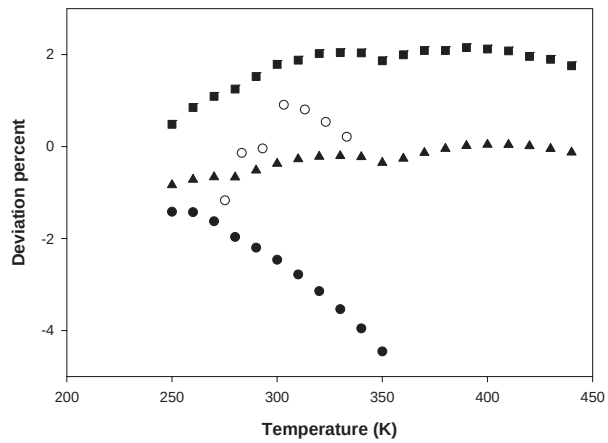


Fig. 6. Deviation plot for the viscosity coefficients of R152a gaseous system at different temperatures compared with experiment: Krauss et al.[26] (■), Lemmon et al.[33] (▲), Grebenkov et al.[47] (●), Assael and Polimatidou[49] (○).

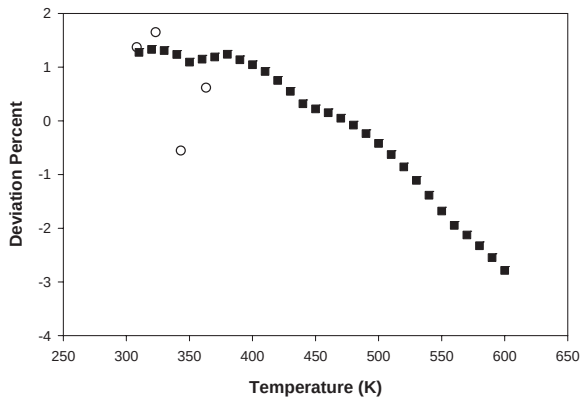


Fig. 7. Deviation plot for the viscosity coefficients of R123 gaseous system at different temperatures compared with experiment: Lemmon et al.[33] (■), Dowdell and Matthews.[46] (○).

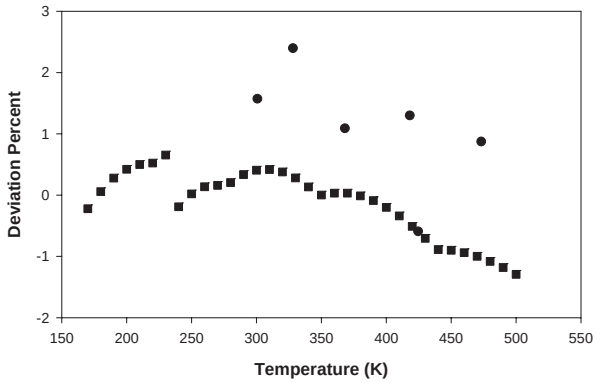


Fig. 8. Deviation plot for the viscosity coefficients of R22 gaseous system at different temperatures compared with experiment: Lemmon et al.[33] (■), Kestin and Wakeham[50] (●).

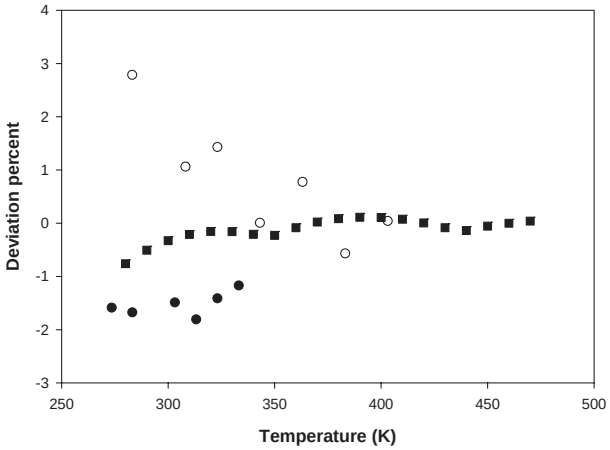


Fig. 9. Deviation plot for the viscosity coefficients of R124 gaseous system at different temperatures compared with experiment: Lemmon et al.[33] (■), Dowdell and Matthews[46] (○), Assael and Polimatidou[49] (●).

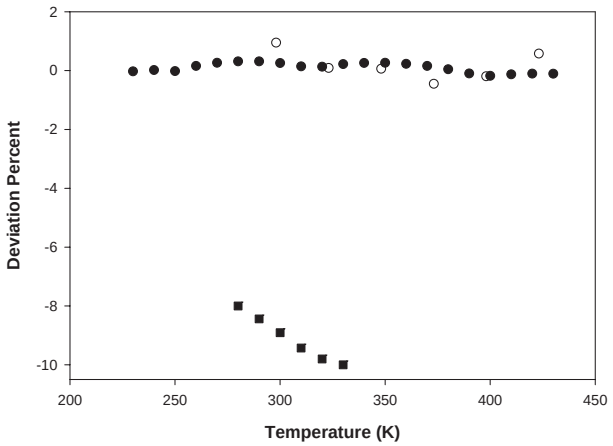


Fig. 10. Deviation plot for the viscosity coefficients of R32 gaseous system at different temperatures compared with experiment: Lemmon et al.[33] (●), Grebenkov et al.[47] (■), Shibasaki-Kitakawa et al.[51] (○).

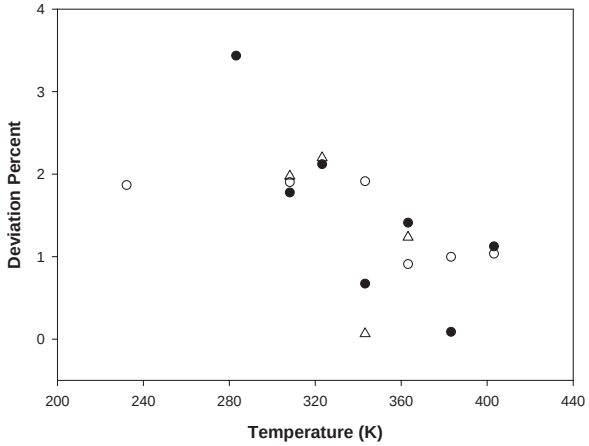


Fig. 11. Deviation plot for the self diffusion coefficients of R134a (○), R123 (△), and R124 (●) gaseous systems at different temperatures compared with experiment: Dowdell and Matthews.[46]

Table 16. Least-Squares Coefficients, Correlation Coefficients ($R$), and Standard Errors (SE) for Eq. 28

| Refrigerant | $a_D$ | $b_D$/K | $c_D$ | $R$ | SE |
|---|---|---|---|---|---|
| Methane | 1.6347221 | −69.24027 | −10.583893 | 0.9999995 | 0.0005466 |
| Ethane | 1.6730771 | −79.926836 | −11.560963 | 0.9999954 | 0.0007752 |
| Propane | 1.6044846 | −151.00028 | −11.442384 | 0.9998797 | 0.0026225 |
| Butane | 2.0826047 | 81.241835 | −15.262456 | 0.99996895 | 0.0009827 |
| R134a | 1.6510726 | −107.96681 | −12.341485 | 0.9999961 | 0.0002738 |
| R152a | 1.6932449 | −109.07891 | −12.282 | 0.9999937 | 0.0004944 |
| R123 | 1.6515749 | −106.50092 | −12.848928 | 0.9999957 | 0.0001746 |
| R22 | 1.6899674 | −108.91256 | −12.315646 | 0.9999929 | 0.0004979 |
| R143a | 1.6449112 | −105.74995 | −12.033427 | 0.9999962 | 0.0003563 |
| R124 | 1.6506411 | −105.95048 | −12.640045 | 0.9999955 | 0.0002175 |
| R32 | 1.676982 | −105.42003 | −11.74606 | 0.9999956 | 0.0006314 |

range of 200 K $< T <$ 1000 K using Eqs. 19–22 reported by Huber et al.[10] The predicted values of thermal conductivities for all studied refrigerants are tabulated in Tables 4–14. The calculated thermal conductivities were correlated with the following equation:

$$\lambda = a_\lambda + b_\lambda T + c_\lambda T^2 + d_\lambda T^3. \quad (30)$$

Table 17. Least-Squares Coefficients, Correlation Coefficients ($R$), and Standard Errors (SE) for Eq. 29

| Refrigerant | $a_\alpha$ | $b_\alpha/K^{-1}$ | $c_\alpha/K^{-2}$ | $d_\alpha/K^{-3}$ | $e_\alpha/K^{-4}$ | $R$ | SE |
|---|---|---|---|---|---|---|---|
| Methane | −0.2242446 | 0.0022232 | −2.66099E-0006 | 1.43778E-009 | −2.6813E-013 | 0.999974 | 0.0009437 |
| Ethane | −0.0625459 | 0.0002966 | 1.884956E-006 | −2.91139E-009 | 1.24503E-012 | 0.999964 | 0.0011966 |
| Propane | 0.0275345 | −0.0003665 | 2.309877E-006 | −2.47692E-009 | 8.63153E-013 | 0.9999745 | 0.0008206 |
| Butane | −0.0349848 | 0.0001471 | 2.573122E-007 | 4.60221E-011 | −1.39311E-013 | 0.999951 | 0.0009018 |
| R134a | −0.1258469 | −0.0001732 | 3.722384E-006 | −5.11282E-009 | 2.12719E-012 | 0.9997878 | 0.0035437 |
| R152a | 0.1308295 | −0.0021467 | 7.857447E-006 | −8.84552E-009 | 3.38338E-012 | 0.999731 | 0.0036533 |
| R123 | −0.1350951 | −6.6238E-0 | 3.441361E-006 | −4.80328E-009 | 2.00369E-012 | 0.9998343 | 0.0031275 |
| R22 | 0.1041227 | −0.0019451 | 7.406856E-006 | −8.39975E-009 | 3.21849E-012 | 0.999720 | 0.0037718 |
| R143a | −0.1744293 | 0.0002683 | 2.71819E-009 | −4.15211E-009 | 1.78915E-012 | 0.9998602 | 0.0028854 |
| R124 | −0.129233 | −0.0001375 | 3.775581E-006 | −5.30138E-009 | 2.23685E-012 | 0.999744 | 0.0039023 |
| R32 | −0.0243361 | −0.00101160 | 5.522446E-006 | −6.7799E-009 | 2.70700E-012 | 0.999856 | 0.0028422 |

Table 18. Least-Squares Coefficients, Correlation Coefficients ($R$), and Standard Errors (SE) for Eq. 30

| Refrigerant | $\mathbf{a}_\lambda$ (mw/mk) | $\mathbf{b}_\lambda$ (mw/mk$^2$) | $\mathbf{c}_\lambda$ (mw/mk$^3$) | $\mathbf{d}_\lambda$ (mw/mk$^4$) | $R$ | SE |
|---|---|---|---|---|---|---|
| Methane | 9.4120503 | 0.02391513 | 0.00023797 | −9.86290E-008 | 0.999997 | 0.111502 |
| Ethane | 2.1541664 | 0.00575251 | 0.00024687 | −1.15970E-007 | 0.999974 | 0.292932 |
| Propane | 0.9216463 | 5.729E-005 | 0.00023678 | −1.0995E-007 | 0.999983 | 0.217426 |
| Butane | 4.5623104 | −0.01670239 | 0.00023807 | −1.05898E-007 | 0.999972 | 0.264329 |
| R134a | −4.1935875 | 0.04130039 | 7.569E-005 | −4.73937E-008 | 0.999946 | 0.199641 |
| R152a | −1.0033528 | 0.01555113 | 0.00014438 | −7.47704E-008 | 0.999974 | 0.179062 |
| R123 | −3.5665573 | 0.03624247 | 3.557E-005 | −2.55192E-008 | 0.999956 | 0.115893 |
| R22 | −1.8985696 | 0.02677853 | 7.141E-005 | −4.18462E-008 | 0.999962 | 0.137170 |
| R143a | −4.9481381 | 0.04850531 | 9.386E-005 | −5.58845E-008 | 0.999953 | 0.231612 |
| R124 | 1.7531669 | −0.00726093 | 0.00016852 | −1.22000E-007 | 0.000089 | 0.063961 |
| R32 | 19.267534 | −0.13560243 | 0.00050764 | −3.61086E-007 | 0.999530 | 0.499197 |

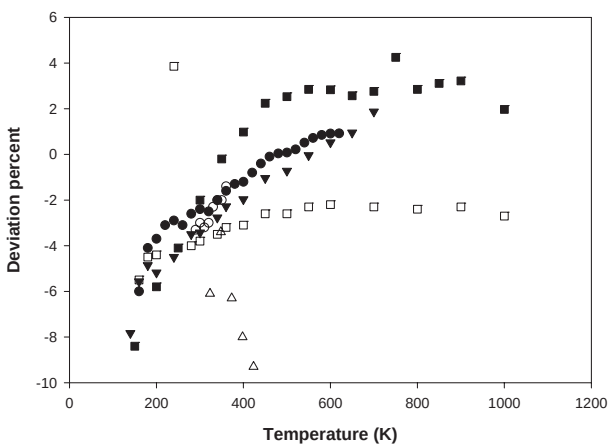


Fig. 12. Deviation plot for the thermal conductivities of methane gaseous system compared with experiment: Vargaftik et al.[29] (□), Smith et al.[30] (△), Lemmon et al.[33] (●), Heckenberger and Stephan[37] (▼), Patek and Klomfar[54] (○), Assael et al.[55] (■).

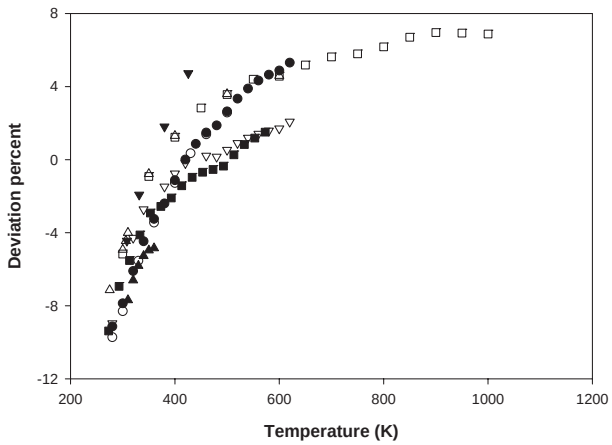


Fig. 13. Deviation plot for the thermal conductivities of ethane gaseous system compared with experiment: Vargaftik et al.[29] (■), Lemmon et al.[33] (●), Heckenberger and Stephan[37] (▽), Friend et al.[39] (○), Hendle et al.[40] (□), Vesovic et al.[56] (△), Desmart and Tufeu[57] (▲), Millat et al.[58] (▼).

Parameters in the above equation were allowed to vary for each system using non-linear least-squares method and are listed in Table 18 along with $R$ and SE for each refrigerant.

At this juncture, it should be added that the heat capacity at a constant pressure, a quantity necessary for calculating internal contributions to the thermal conductivity, were taken from Assael et al.[52] for R32 and R124 and from Poling et al.[53] for the remaining refrigerants. Because the heat capacities were valid in the temperature range of $50\,K < T < 1000\,K$, we focused our effort to predicting thermal conductivities confined to the aforementioned temperature range.

Typical deviations of the experimental thermal conductivities[29,30,33,37,39,40,54–62] of methane, ethane, propane, and butane are plotted in Figs. 12–15. In the specific case of methane, the calculated thermal conductivities agree with the ones reported by NIST (Lemmon et al.[33]), those published by Patek and

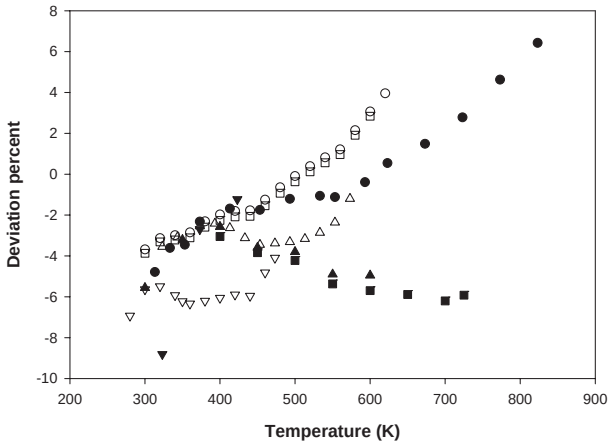


Fig. 14. Deviation plot for the thermal conductivities of propane gaseous system compared with experiment: Vargaftik et al.[29] (●), Smith et al.[30] (▼), Lemmon et al.[33] (○), Heckenberger and Stephan[37] (▽), Aggarwal and Springer[59] (■), Ramires et al.[60] (▲), Tufeu and Le Neindre[61] (△), Marsh et al.[62] (□).

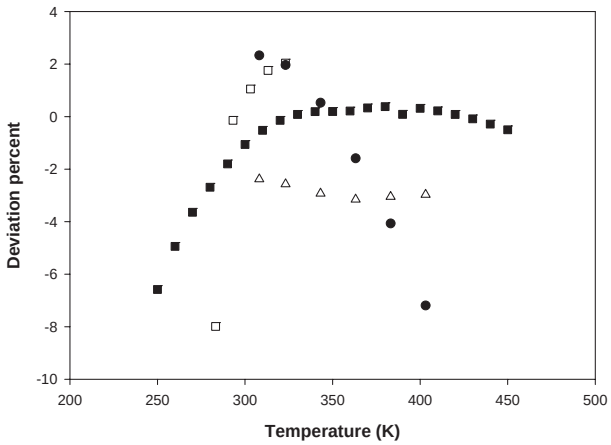


Fig. 16. Deviation plot for the thermal conductivities of R134a gaseous system compared with experiment: Huber et al.[10] (●), Lemmon et al.[33] (■), Grebenkov et al.[47] (△), Assael et al.[63] (□).

Klomfar[54] and those obtained by Assael et al.[55] within a 3% error range. In contrast, they deviate from those given by Vargaftik et al.[29] and Smith et al.[30] in 4% and 6% error ranges, respectively. Meanwhile, the predicted thermal conductivities for propane are in good agreement (accuracies of 4%) with those reported by Lemmon et al.[33] and by Marsh et al.[62] These last two are thought to be the most reliable values of the thermal conductivities pertinent to this system.

A comparison has also been made between the predicted thermal conductivities of R134a, R152a, R22, and R124 with those found in the literature[10,26,29,33,37,47,63] in Figs. 16–19, respectivley. It should be mentioned that Huber and his co-workers have modified their method using $f_{int}$ in Eq. 20 as a simple temperature dependent function. We employed their recent work and predicted the thermal conductivities of the refrigerants R32 and R124. The results are shown in Fig. 20. Furthermore, for completeness, shown for comparison are the predicted thermal conductivities of these systems from the previous

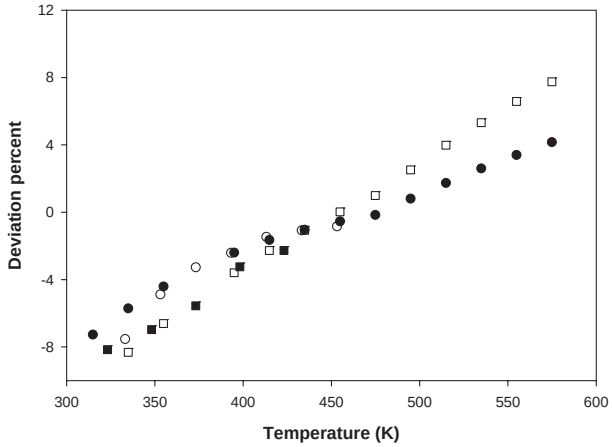


Fig. 15. Deviation plot for the thermal conductivities of butane gaseous system compared with experiment: Vargaftik et al.[29] (○), Smith et al.[30] (■), Lemmon et al.[33] (●), Heckenberger and Stephan[37] (□).

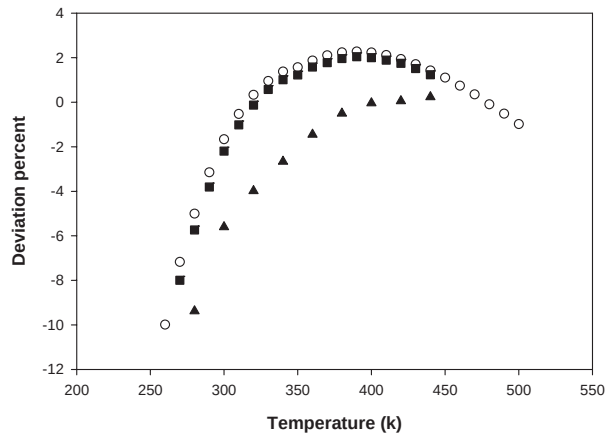


Fig. 17. Deviation plot for the thermal conductivities of R152a gaseous system at different temperatures compared with experiment: Krauss et al.[26] (■), Vargaftik et al.[29] (▲), Lemmon et al.[33] (○).

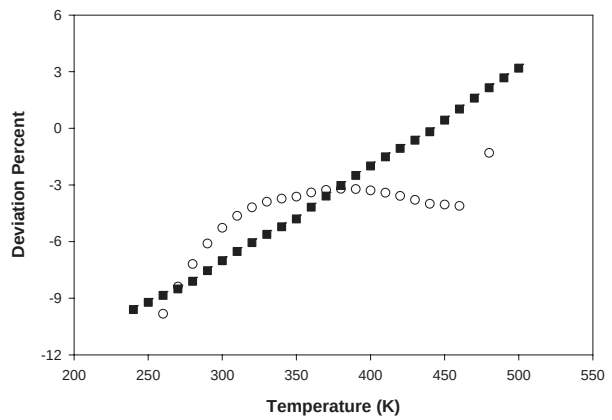


Fig. 18. Deviation plot for the thermal conductivities of R22 gaseous system at different temperatures compared with experiment: Lemmon et al.[33] (■), Heckenberger and Stephan[37] (○).

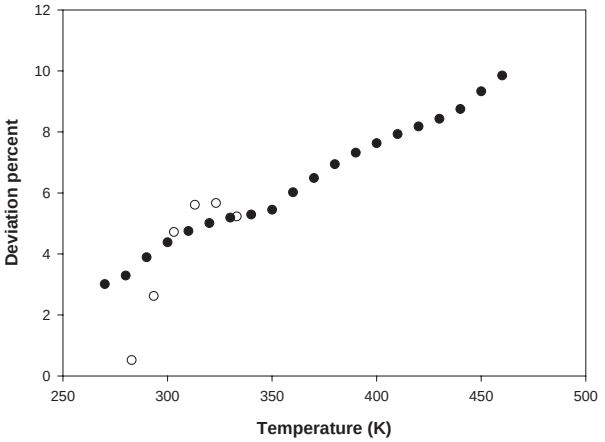


Fig. 19. Deviation plot for the thermal conductivities of R124 gaseous system at different temperatures compared with experiment: Lemmon et al.[33] (●), Assael et al.[63] (○).

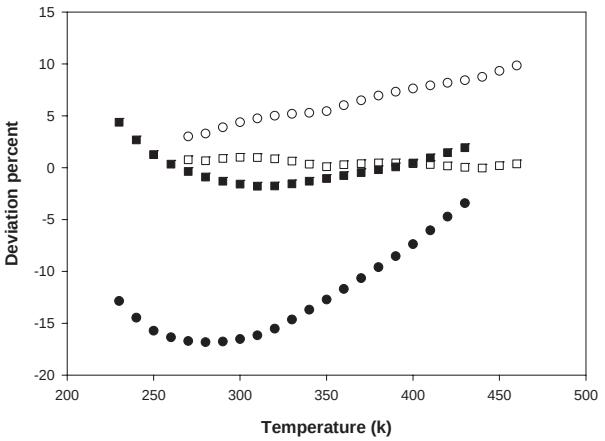


Fig. 20. Deviation plot for the thermal conductivities of R32 and R124 obtained from Huber's methods, compared with the literature[33] [R32 (●)–R124 (○)],[11] [R32 (■)–R124 (□)].[12]

Huber's method.[10] We found that the predicted thermal conductivites using the modified scheme[11] deviated from the literature data[33] with a maximum error of 5%, whereas the accuracies of the previous model[10] within a 10% error range. It is worth stressing that the calculations were restricted to two refrigerants, R32 and R124, because Huber et al.[11] do not report the coefficients of $f_{int}$ for the other refrigerants.

In general, the collective results of this work show in a convincing manner that the original Huber method[10] and especially their modified method[11] is a promising approach for computing thermal conductivities of pure refrigerants, including light hydrocarbons and their halogenated analogues.

## Conclusion

As remarked earlier, in order to use optimally, accurate and reliable knowledge of viscosity as well as other thermophysical properties of refrigerants is needed. The wide range of refrigerants and conditions of interest precludes obtaining the relevant data by experimental means alone; thus, the development of prediction methods is required.

The present work as well as the previous works shows that inversion procedure is both a powerful method for generating energy from the law of corresponding states of viscosity and a valuable supplement for obtaining transport properties, especially at high or low temperatures where direct measurements are practically difficult. In addition to being able to predict the viscosity with an acceptable accuracy, our inverted pair potential energies could be used to determine other transport properties, such as thermal conductivity and self diffusion coefficient with acceptable accuracies. Moreover, for the first time, this method was employed to predict transport properties of refrigerants, which are rather polar molecules.

It was also found that the modified Huber method in comparison to the original work reduces the errors in the calculated thermal conductivities to within 5%.

The authors wish to express to Research Committees of Shiraz University and Shiraz University of Technology their sincere thanks for supporting this project and making computer facilities available.

## References

1 A. S. Teja, R. L. Smith, Jr., R. K. King, T. F. Sun, *Int. J. Thermophys.* **1999**, *20*, 149.
2 M. J. P. Comuñas, A. Baylaucq, S. E. Quiñones-Cisneros, C. K. Zeberg-Mikkelssen, C. Boned, J. Ferńandez, *Fluid Phase Equilib.* **2003**, *210*, 21.
3 M. Fermeglia, M. Ferrone, S. Pricl, *Fluid Phase Equilib.* **2003**, *210*, 105.
4 J. Moghadasi, D. Mohammad-Aghaie, M. M. Papari, *Ind. Eng. Chem. Res.* **2006**, *45*, 9211.
5 M. M. Papari, *Chem. Phys.* **2003**, *288*, 249.
6 J. Moghadasi, M. M. Papari, A. Nekoie, J. V. Sengers, *Chem. Phys.* **2004**, *306*, 229.
7 M. M. Papari, D. Mohammad-Aghaiee, B. Haghighi, A. Boushehri, *Fluid Phase Equilib.* **2005**, *232*, 122.
8 S. Sheikh, M. M. Papari, A. Boushehri, *Ind. Eng. Chem. Res.* **2002**, *41*, 3274.
9 M. M. Papari, A. Razavizadeh, F. Mokhberi, A. Boushehri, *Ind. Eng. Chem. Res.* **2003**, *42*, 3802.
10 M. L. Huber, D. G. Friend, J. F. Ely, *Fluid Phase Equilib.* **1992**, *80*, 249.
11 M. L. Huber, A. Laesecke, R. Perkins, *Ind. Eng. Chem. Res.* **2003**, *42*, 3163.
12 S. Chapman, T. G. Cowling, *The Mathematical Theory of Non-Uniform Gases*, Cambridge University Press, London, **1970**.
13 J. O. Hirschfelder, C. F. Curtiss, R. B. Bird, *Molecular Theory of Gases and Liquids*, John Wiley, New York, **1964**.
14 L. Monchick, E. A. Mason, *J. Chem. Phys.* **1961**, *35*, 1676.
15 A. Boushehri, J. Bzowski, J. Kestin, E. A. Mason, *J. Phys. Chem. Ref. Data* **1987**, *16*, 445.
16 R. B. Bird, W. E. Stewart, E. N. Lightfoot, *Transport Phenomena*, Wiley, New York, **2002**.
17 A. Boushehri, *Physica A* **1979**, *97*, 206.
18 M. M. Papari, A. Boushehri, *Bull. Chem. Soc. Jpn.* **1998**, *71*, 2757.
19 M. M. Papari, D. Mohammad-Aghaie, J. Moghadasi, A. Boushehri, *Bull. Chem. Soc. Jpn.* **2006**, *79*, 67.
20 L. A. Monchick, *J. Chem. Phys.* **1980**, *73*, 2929.
21 J. P. M. Trusler, *Mol. Phys.* **1988**, *64*, 1153.
22 L. A. Viehland, E. A. Mason, W. F. Morrison, M. R.

Flannery, *Atom. Data Nucl. Data Tables* **1975**, *16*, 495.
23 B. Najafi, Y. Ghayeb, G. A. Parsafar, *Int. J. Thermophys.* **2000**, *21*, 1011.
24 P. D. Neufeld, A. R. Janzen, R. A. Aziz, *J. Chem. Phys.* **1972**, *57*, 1100.
25 H. Nabizadeh, F. Mayinger, *High Temp.-High Pressures* **1992**, *24*, 221.
26 R. Krauss, V. C. Weiss, T. A. Edison, J. V. Sengers, K. Stephan, *Int. J. Thermophys.* **1996**, *17*, 731.
27 M. Rigby, E. B. Smith, W. A. Wakeham, G. C. Maitland, *The Forces between Molecules*, Clarendon Press, Oxford, **1986**.
28 Y. Abe, J. Kestin, H. E. Khalifa, W. A. Wakeham, *Physica A* **1978**, *93*, 155.
29 N. B. Vargaftik, Y. K. Vinogradov, V. S. Yargin, *Handbook of Physical Properties of Liquids and Gases*, Begell House Inc., New York, **1996**.
30 W. J. S. Smith, L. D. Durbin, R. Kobayashi, *J. Chem. Eng. Data* **1960**, *5*, 316.
31 R. D. Trengove, W. A. Wakeham, *J. Phys. Chem. Ref. Data* **1987**, *16*, 175.
32 J. J. Hurly, K. A. Gillis, J. B. Mehl, M. R. Moldover, *Int. J. Thermophys.* **2003**, *24*, 1441.
33 E. W. Lemmon, M. O. Mclinden, D. G. Friend, in *Thermophysical Properties of Fluid Systems in NIST Chemistry Webbook, NIST Standard Reference Database Number 69*, ed. by W. G. Mallard, P. J. Linstrom, November, **1998**, Nat. Inst. Stand. Tech., Gaithersburg, MD20899, http://webbook.nist.gov.
34 C. Evers, H. W. Lösch, W. Wagner, *Int. J. Thermophys.* **2002**, *23*, 1411.
35 P. Schley, M. Jaeschke, C. Küchenmeister, E. Vogel, *Int. J. Thermophys.* **2004**, *25*, 1623.
36 J. Kestin, H. E. Khalifa, W. A. Wakeham, *J. Chem. Phys.* **1977**, *66*, 1132.
37 T. Heckenberger, K. Stephan, *Int. J. Thermophys.* **1991**, *12*, 333.
38 H. Iwasaki, M. Takahashi, *J. Chem. Phys.* **1981**, *74*, 1930.
39 D. G. Friend, H. Ingham, J. F. Ely, *J. Phys. Chem. Ref. Data* **1991**, *20*, 275.
40 S. Hendl, J. Millat, E. Vogel, V. Vesovic, W. A. Wakeham, L. Luttmer-Strathmann, J. V. Sengers, M. J. Assael, *Int. J. Thermophys.* **1994**, *15*, 1.
41 S. Hendl, J. Millat, V. Vesovic, E. Vogel, W. A. Wakeham, *Int. J. Thermophys.* **1991**, *12*, 999.
42 J. Wilhelm, E. Vogel, *Int. J. Thermophys.* **2000**, *21*, 301.
43 E. Vogel, C. Kuchenmeister, E. Bich, *J. Phys. Chem. Ref. Data* **1998**, *27*, 947.
44 C. Kuchenmeister, E. Vogel, *Int. J. Thermophys.* **1998**, *19*, 1085.
45 Y. Abe, J. Kestin, H. E. Khalifa, W. A. Wakeham, *Physica A* **1979**, *97*, 296.
46 D. C. Dowdell, G. P. Matthews, *J. Chem. Soc., Faraday Trans.* **1993**, *89*, 3545.
47 A. J. Grebenkov, V. P. Zhelezny, P. M. Klepatsky, O. V. Beljajeva, Y. A. Chernjak, Y. G. Kotelevsky, B. D. Timofejev, *Int. J. Thermophys.* **1996**, *17*, 535.
48 *Transport Properties of Fluids: Their Correlation, Estimation and Prediction*, ed. by J. Millat, J. H. Dymond, C. A. Nieto de Castro, Cambridge University Press, Cambridge, **1996**.
49 M. J. Assael, S. K. Polimatidou, *Int. J. Thermophys.* **1997**, *18*, 353.
50 J. Kestin, W. A. Wakeham, *Ber Bunsen-Ges. Phys. Chem.* **1979**, *83*, 573.
51 N. Shibasaki-Kitakawa, M. Takahashi, C. Yokoyama, S. Takahashi, *J. Chem. Eng. Data* **1995**, *40*, 900.
52 M. J. Assael, J. P. M. Trusler, T. F. Tsolakis, *An Introduction to Their Prediction: Thermophysical Properties of Fluids*, Imperial College Press, London, **1996**.
53 B. E. Poling, J. M. Prausnitz, J. P. O'Connell, *The Properties of Gases and Liquids*, McGraw-Hill, New York, **2001**.
54 J. Pátek, J. Klomfar, *Fluid Phase Equilib.* **2002**, *198*, 147.
55 M. J. Assael, J. Millat, V. Vesovic, W. A. Wakeham, *J. Phys. Chem. Ref. Data* **1990**, *19*, 1137.
56 V. Vesovic, W. A. Wakeham, J. Luettmer-Strathmann, J. V. Sengers, J. Millat, E. Vogel, M. J. Assael, *Int. J. Thermophys.* **1994**, *15*, 33.
57 P. Desmarest, R. Tufeu, *Int. J. Thermophys.* **1987**, *8*, 293.
58 J. Millat, M. Ross, W. A. Wakeham, M. Zalaf, *Int. J. Thermophys.* **1988**, *9*, 481.
59 M. C. Aggarwal, G. S. Springer, *J. Chem. Phys.* **1979**, *70*, 3948.
60 M. L. V. Ramires, C. A. Nieto de Castro, R. A. Perkins, *Int. J. Thermophys.* **2000**, *21*, 639.
61 R. Tufeu, R. B. Le Neindre, *Int. J. Thermophys.* **1987**, *8*, 27.
62 K. N. Marsh, R. A. Perkins, M. L. V. Ramires, *J. Chem. Eng. Data* **2002**, *47*, 932.
63 M. J. Assael, M. Malamataris, L. Karagiannidis, *Int. J. Thermophys.* **1997**, *18*, 341.